Correction

APPLIED PHYSICAL SCIENCES, NEUROSCIENCE

Correction for "Bioelectronic neural pixel: Chemical stimulation and electrical sensing at the same site," by Amanda Jonsson, Sahika Inal, Ilke Uguz, Adam J. Williamson, Loïg Kergoat, Jonathan Rivnay, Dion Khodagholy, Magnus Berggren, Christophe Bernard, George G. Malliaras, and Daniel T. Simon, which appeared in issue 34, August 23, 2016, of *Proc Natl Acad Sci USA* (113:9440–9445; first published August 9, 2016; 10.1073/pnas.1604231113).

The authors note that, due to a printer's error, the first name of the third author, Ilke Uguz, originally published with the first letter as a lowercase letter *l*. This letter should instead appear as an uppercase letter *i*. The online version has been corrected.

www.pnas.org/cgi/doi/10.1073/pnas.1615817113

CORRECTION

Bioelectronic neural pixel: Chemical stimulation and electrical sensing at the same site

Amanda Jonsson[a,1], Sahika Inal[b,1], Ilke Uguz[b,1], Adam J. Williamson[c,1], Loïg Kergoat[a,c], Jonathan Rivnay[b,2], Dion Khodagholy[b,3], Magnus Berggren[a], Christophe Bernard[c], George G. Malliaras[b], and Daniel T. Simon[a,4]

[a]Laboratory of Organic Electronics, Department of Science and Technology, Linköping University, 60174 Norrköping, Sweden; [b]Department of Bioelectronics, École Nationale Supérieure des Mines de Saint-Etienne, Centre Microélectronique de Provence, Microelectronique et Objects Communicants, 13541 Gardanne, France; and [c]Aix Marseille Université, Institut de Neurosciences des Systèmes, 13005 Marseille, France

Edited by Zhenan Bao, Stanford University, Stanford, California, and accepted by Editorial Board Member John A. Rogers June 27, 2016 (received for review March 14, 2016)

Local control of neuronal activity is central to many therapeutic strategies aiming to treat neurological disorders. Arguably, the best solution would make use of endogenous highly localized and specialized regulatory mechanisms of neuronal activity, and an ideal therapeutic technology should sense activity and deliver endogenous molecules at the same site for the most efficient feedback regulation. Here, we address this challenge with an organic electronic multifunctional device that is capable of chemical stimulation and electrical sensing at the same site, at the single-cell scale. Conducting polymer electrodes recorded epileptiform discharges induced in mouse hippocampal preparation. The inhibitory neurotransmitter, γ-aminobutyric acid (GABA), was then actively delivered through the recording electrodes via organic electronic ion pump technology. GABA delivery stopped epileptiform activity, recorded simultaneously and colocally. This multifunctional "neural pixel" creates a range of opportunities, including implantable therapeutic devices with automated feedback, where locally recorded signals regulate local release of specific therapeutic agents.

organic electronics | controlled delivery | electrophysiology | epilepsy | therapy

Recent estimates suggest neurological disorders affect up to 6% of the global population (1). The vast majority of treatments generally involve oral administration of pharmaceuticals. When these fail, alternate therapies can include neurosurgery (e.g., in epilepsy) and electrical stimulation via implanted electrodes [e.g., in Parkinson's disease (1)]. Pharmaceutical and basic research have identified promising targets and designed potentially efficient drugs for multiple disorders, but such drugs haven't reached patients because of failure during (pre)clinical tests. There are multiple reasons for such failures. Drugs may be toxic in the periphery (2, 3), they may not cross the blood–brain barrier or they may be pumped back to the blood stream by multidrug transporters (4, 5). However, the critical factor is the fact that they may have deleterious side effects when they penetrate "healthy" regions, affecting physiological functions such as memory and learning (6, 7). In addition, because oral administration will lead to a dilution of the drug in the body, there is often a mismatch between the dose necessary to obtain a therapeutic effect in the region to treat and the maximum dose that nonaffected body regions can support without side effects.

Providing the drug past the blood–brain barrier, where and when it is needed, constitutes the ideal solution. Such delivery would solve all of the above-mentioned problems (blood–brain barrier crossing, peripheral toxicity, undesirable side effects in healthy regions, and effective dose). Devices have been successfully designed to deliver drugs locally (8). However, the "where" and "when" issues remain to be addressed. Because clinicians may have several spatially distributed regions to treat, or if the volume of the intended treatment region is large, it is important to have multiple drug delivery sites, which would solve the "where" issue. The "when" issue is more difficult to address, as, ideally, a delivery system should act on demand, when needed (e.g., just before an impending seizure). Because electrophysiological signals can be used to predict incoming pathological events (9), electrical activity should be measured at each delivery site to trigger drug delivery at that specific location. Such local, real-time measurement, and precision delivery, would pave the way for closed-loop, fully automatic, therapeutic devices. Finally, because the size of the region to treat may be small—down to the scale of a single cell—the technology should allow spatial resolution of delivery on the order of micrometers.

Interfacing malfunctioning neurological pathways with spatial resolution and signal specificity approaching those of the cell could provide significant advantages to future therapies. Microelectrode recordings of the field potentials generated by neurons (or even neuronal firing itself) have become routine in investigations of brain function and dysfunction (10). Small size of recording sites allows for recording of single neurons, and densely packed sites on minimally invasive electrodes enhance the sampling capacity of the probe (11). Such densely packed probes can be accomplished using conducting polymers, such as poly(3,4-ethylenedioxythiophene) doped with poly(styrenesulfonate) (PEDOT:PSS), without decreasing the quality of the recordings. Conducting polymer electrodes exhibit inherently low impedance characteristics (more than

Significance

Electronically and ionically conducting polymers provide a unique means to translate electronic addressing signals into chemically specific and spatiotemporally resolved delivery, without fluid flow. These materials have also been shown to provide high-fidelity electrophysiological recordings. Here, we demonstrate the combination of these qualities of organic electronics in multiple 20 × 20 μm delivery/sensing electrodes. The system is used to measure epileptic activity in a brain slice model, and to deliver inhibitory neurotransmitters to the same sites as the recordings. These results show that a single-cell-scale electrode has the ability to both record and chemically stimulate, demonstrating the local effects of therapeutic treatment, and opening a range of opportunities in basic neuroscience as well as medical technology development.

Author contributions: A.J., S.I., I.U., A.J.W., L.K., J.R., D.K., M.B., C.B., G.G.M., and D.T.S. designed research; A.J., S.I., I.U., A.J.W., and L.K. performed research; A.J., S.I., I.U., A.J.W., L.K., and C.B. analyzed data; and A.J., S.I., and D.T.S. wrote the paper.

The authors declare no conflict of interest.

This article is a PNAS Direct Submission. Z.B. is a Guest Editor invited by the Editorial Board.

[1]A.J., S.I., I.U., and A.J.W. contributed equally to this work.

[2]Present address: Electronic Materials and Devices Lab, Palo Alto Research Center, Palo Alto, CA 94304.

[3]Present address: Neuroscience Institute, School of Medicine, New York University, New York, NY 10016.

[4]To whom correspondence should be addressed. Email: daniel.simon@liu.se.

This article contains supporting information online at www.pnas.org/lookup/suppl/doi:10.1073/pnas.1604231113/-/DCSupplemental.

www.pnas.org/cgi/doi/10.1073/pnas.1604231113

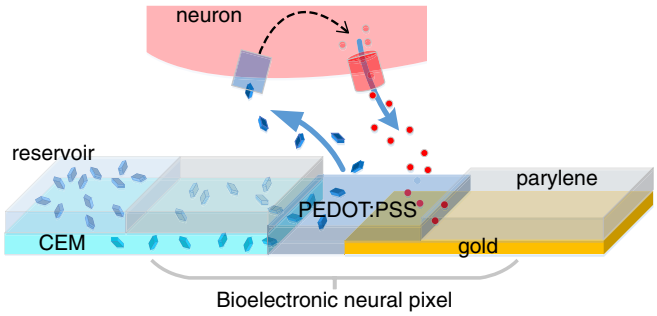

Fig. 1. The bioelectronic neural pixel. The OEIP channel outlet (terminating in the PEDOT:PSS) colocalized with the PEDOT:PSS recording electrode forms one neural pixel. The reservoir (left) comprises an aqueous solution of the positively charged compound to be delivered through the CEM and out through the PEDOT:PSS recording electrode to the neural tissue above the pixel. The biological response, in terms of ion fluxes, is measured locally by the PEDOT:PSS recording electrode colocalized with the OEIP outlet.

one order of magnitude lower than bare Au, Pt, and Ir electrodes of similar dimensions at 1 kHz), with the low impedance being attributed partly to the high porosity, giving an increased electrochemical surface area (12–14). Additionally, with their mixed electronic and ionic conductivity and the soft mechanical properties that match those of the neural tissue, conducting polymers are ideally suited to obtain high signal-to-noise ratio recordings at the neural interface (15, 16). Recently, we have demonstrated microelectrode arrays based on PEDOT:PSS electrodes for in vitro recordings of electrophysiological signals from rat brain slices (17). These microelectrodes, fabricated at small size and high density, have enabled a good match with the dimensions of neural networks while maintaining high-resolution neural recordings.

We have also demonstrated substance delivery mimicking exocytotic release of neurotransmitters at the neuronal scale by means of the organic electronic ion pump (OEIP) (18, 19). The OEIP uses conducting polymer electrodes to electrophoretically "pump" neurotransmitters through a permselective membrane, enabling high spatiotemporal delivery resolution, without necessitating liquid flow. OEIPs have been used in vitro to trigger cell signaling (18, 20) and to control epileptiform activity in vitro (21), as well as in vivo to effect sensory function (19) and as a therapy for pain in awake animals (22). OEIPs have also been demonstrated in a biosensor-regulated system—on a macroscopic scale—to mimic the chemical-to-electrical-to-chemical signal transduction of neurons (23). However, none of these devices meet the desired requirement to record and deliver drugs at the same site.

In this work, we engineered a device able to perform electrical sensing of local field potentials and neurotransmitter delivery at the same site. To achieve this colocalized sensing and delivery, we developed a system consisting of an array of OEIP delivery points, where each delivery point is integrated with a conducting polymer electrode for recording neuronal activity. Each integrated delivery/sensing pixel is at the single-cell scale and mimics the multifunctionality of a biological neuron: Electrical information can be sensed from the local cellular environment, and neuroactive compounds can be delivered diffusively, without liquid flow, at the same location. We report on the development and characterization of this system of "neural pixels," and we demonstrate its use by delivering the endogenous inhibitory neurotransmitter γ-aminobutyric acid (GABA) to locally affect cells while simultaneously monitoring how the delivery modulates the cells' firing patterns.

Results

Design and Working Principle. We designed our bioelectronic neural pixel as depicted in Fig. 1. The charged compound to be delivered is transported from an aqueous reservoir through a cation-conducting channel and through part of the PEDOT:PSS recording electrode before being released to the biological system. In this way, the cells close to the OEIP outlets are affected by the delivery, and the electrodes can record the subsequent modifications in cellular response. The OEIP transports cations by migration; when a potential is applied between an electrode in the reservoir and an electrode in the medium containing the biological system under study, an electric field is established across the cation-conducting channel, and a current arises from cation migration from the reservoir to the biological system. In this way, delivery is only achieved when nonzero voltage is applied (see On–Off Switching and Leakage in OEIPs for more details). The cation-conducting channel has a high concentration of fixed negative charges and is therefore permeable to cations but not to anions (Donnan exclusion) (24), and is therefore a form of cation exchange membrane (CEM). Ideally, all of the current passed through a CEM, and thus through the device, is due to cation transport, and no anions are transported in the opposite direction; this means that the delivery rate is directly proportional to the current, with 1 μA corresponding to a delivery rate of 10 nmol/s. Sustained delivery (constant current) requires nonpolarizable high-capacity electrodes that can transfer charge between the electrode and the electrolyte. We used PEDOT:PSS electrodes for this purpose, on top of which were placed the source (reservoir) and target electrolytes (Fig. 2*A*). Note that no potential was applied to the recording electrodes at the delivery outlets to control the delivery of ions.

Fabrication and Characterization. The materials and processing of an OEIP and a conducting polymer microelectrode array (MEA) are of similar nature, making it possible to manufacture the two components of the merged device simultaneously on a single glass substrate. To fabricate the bioelectronic neural pixel device, we developed a manufacturing protocol based on standard microfabrication techniques. Device fabrication is depicted Fig. 2*B*. First, gold electrodes were patterned on a glass substrate using photolithography and lift-off. Then the main element of the OEIP, the CEM, made from the polyanion poly(styrene sulfonate-comaleic acid) (PSSA-co-MA) cross-linked with poly (ethylene glycol) (PEG), was deposited. The CEM was photolithographically patterned and dry-etched into a wide channel leading to 32 thinner [and thus higher ionic resistance (22)] parallel channels ending in 20-μm-wide delivery outlets (Fig. S1). Alternatively, the PSS-co-MA/PEG was patterned by peel-off using parylene (*Methods*). A 2-μm-thick parylene layer, providing the insulating coating of the OEIP and the MEA contacts, was deposited. A thin layer of dilute commercial cleaner was applied as an antiadhesive coating, and a second 2-μm-thick parylene layer was deposited. Openings to define the OEIP electrolytes, the microelectrodes, and the contact pads were obtained by further photolithography and plasma etching through the parylene. PEDOT:PSS was then deposited by spin coating, and the second parylene layer was peeled off to define the OEIP electrolytes and the microelectrodes. The 32 resulting neural pixels thus comprised 20 × 20 μm PEDOT:PSS recording electrodes at the delivery end of each PSSA-co-MA-based OEIP channel. In this way, substance delivery was achieved through the PEDOT:PSS recording electrode, such that the delivery outlet and the recording electrode were indeed at the same site (Fig. 1). Finally, a polydimethylsiloxane (PDMS) gasket was cut with openings over the source electrodes, defining the source solution well, and over the 32 neural pixels and target electrode, defining the target solution well (Fig. S2).

To characterize the multifunctional device, we first measured the impedance of the recording electrodes separately, and then while running a delivery current through the OEIP to investigate whether running the delivery current through the recording electrodes affected the electrical properties of the recording

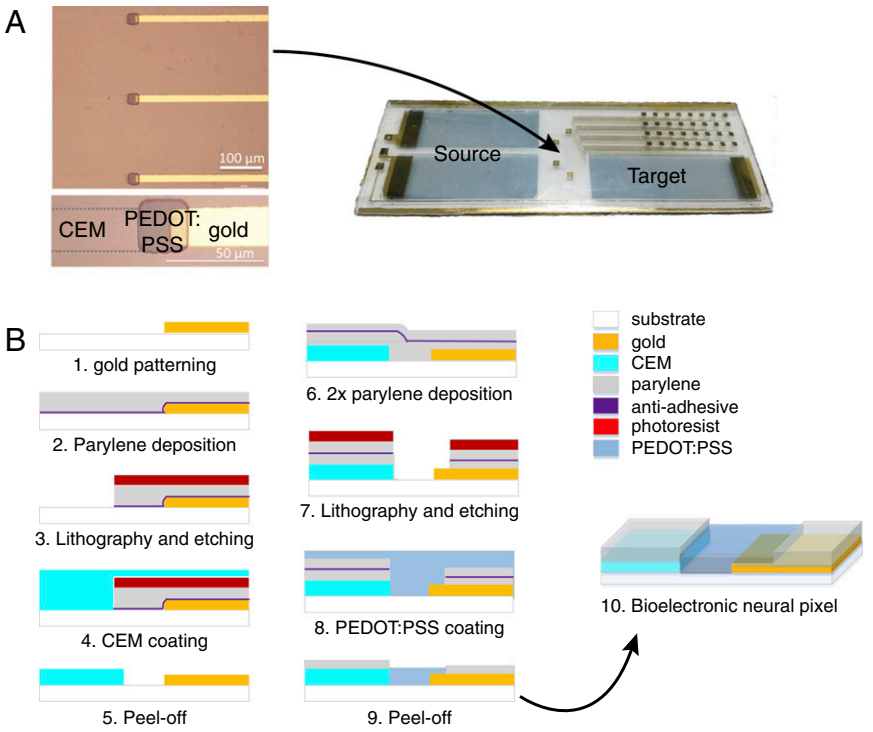

Fig. 2. Design and fabrication of the bioelectronic neural pixel. (*A*) Microscope image of the three adjacent colocalized OEIP outlets and sensing electrodes, and photograph of a typical device. Two source electrodes are depicted, used at equipotential and thus forming effectively one electrode. The reservoir chamber, cut from cured PDMS, is affixed to the source and target areas. The source contains the cation solution to be delivered, and the neural tissue is placed on the target region. Fig. S1 shows the design in more detail. (*B*) Cross-section schematics showing the photolithographic fabrication process. Gold lines were patterned with photolithography (step 1), followed by coating of parylene-C with a thin layer of anti-adhesive (step 2). Photoresist was then cast and exposed, followed by reactive ion etching to define the areas to be filled with CEM (step 3). The CEM [PSSA-co-MA cross-linked with poly(ethylene glycol)] was patterned into a wide channel that split into 32 separate outlets, each 20 µm wide and spaced by 200 µm (Fig. S1), by peeling off the sacrificial top layer of parylene C (steps 4 and 5). Two layers of parylene C were then deposited, separated by a thin layer of antiadhesive (step 6). A thick layer of photoresist was then cast, exposed, and etched to define the areas eventually to be filled with PEDOT:PSS (step 7). A thick layer of PEDOT:PSS (*ca.* 400 nm) was spin-cast (step 8), and the source/target electrodes and the sensing electrodes at the pump outlets were patterned by peeling off the sacrificial top layer of parylene C (step 9). The colocalization of an OEIP outlet with the PEDOT:PSS electrode form a neural pixel (step 10).

electrodes. The Bode plot of the mean impedance magnitude of seven randomly picked PEDOT:PSS electrodes of the array is presented in Fig. 3*A*. The SD of the impedance magnitude is low, indicating that the fabrication process yielded homogeneous electrode properties within the array. Between 10 kHz and 10 Hz, the impedance increased from 16 kΩ to 250 kΩ, and, at 1 kHz, the impedance was *ca.* 19 kΩ, which is similar to our previously reported results (17).

To further investigate the influence of OEIP operation on the signal-to-noise ratio, we compared electrode recordings in the absence and presence of a delivery current (Fig. 3*B*). A 100-mM GABA(aq) solution and artificial cerebrospinal fluid (ACSF) were placed on the source and the target side, respectively. The amplitude of the baseline signal measured when the OEIP was off was *ca.* 10 µV (Fig. 3*B*). After 60 s, a positive potential was applied to the OEIP source electrode with respect to the target, and a current of 1 µA was run through the device, yielding GABA delivery at the 32 outlets. The electrical signal intensity recorded remained stable. The OEIP was switched off after 60 s without apparent change in signal amplitude. A too-high delivery rate could affect the recording electrodes by perturbing the local ion concentration, making cell recordings difficult or impossible. However, as seen in this experiment, constant currents of 1 µA or lower are compatible with electrophysiological recordings.

In Vitro Validation with Complete Hippocampus Preparations: Inhibiting Epileptiform Activity. After confirming that cation delivery did not interfere with electrode recordings, we evaluated sensing and stimulation performance of the pixels in a biological system. As the first application of the integrated device could be for epilepsy diagnosis and treatment, we used complete extracted hippocampus preparations from mouse (P7-P12) and triggered epileptiform activity by pharmacological manipulation, namely the addition of 4-aminopyridine (4-AP) to the perfusion; 4-AP is a selective blocker of channels belonging to the Kv1 family of voltage-gated K^+ channels. Blocking K^+ channels with 4-AP in the perfusion produces epileptiform activity by increasing the time required for a neuron to repolarize (fewer K^+ channels are available). Thus, neurons remain above the threshold to fire for a longer period, and excitatory neurons consequently continue to deliver glutamate to downstream neighbors.

To test the efficacy of the device, we chose to deliver GABA. As an endogenous neurotransmitter, GABA activates $GABA_A$ receptors, leading to Cl^- influx into the cell, which, in turn, hyperpolarizes the cell membrane (Fig. 4*A*). In addition, the opening of these channels decreases the membrane resistance, creating a shunt effect, and limiting the effectiveness of excitatory inputs. The net effect of GABA is therefore a decrease in the firing probability of the cell (25).

With the complete extracted hippocampus preparation mounted (and equilibrated) on the target area of the neural pixel system, we induced epileptiform activity with the addition of 4-AP in the perfusion medium. PEDOT:PSS electrodes recorded the subsequent broadband electrophysiological activity (Fig. 4*B*). The recordings, which were simultaneously obtained via multiple channels, had signal quality comparable to a conventional tungsten recording

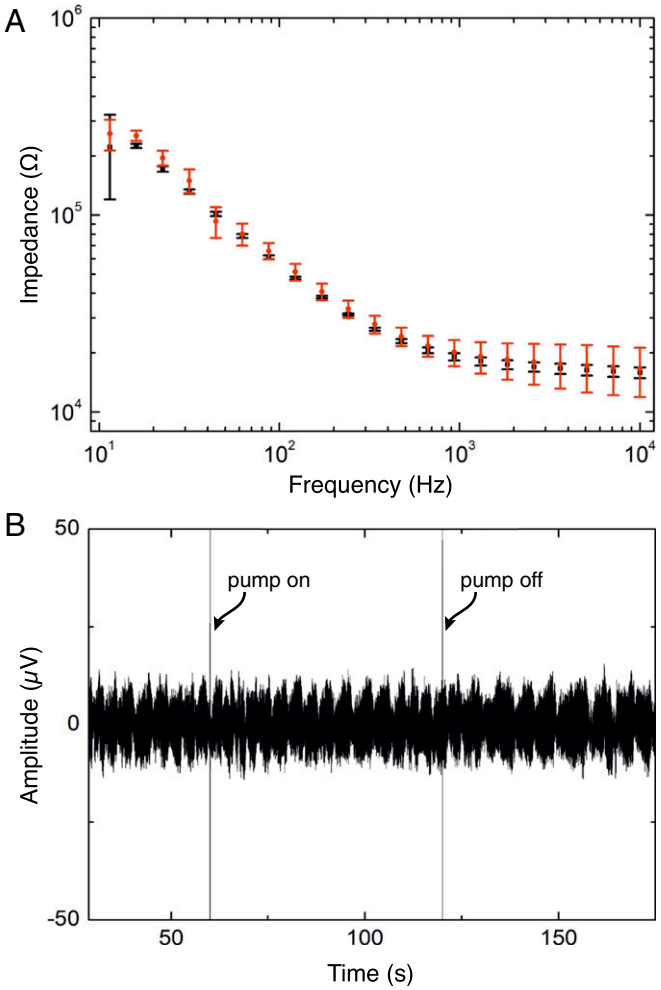

Fig. 3. Characterization of sensing electrodes incorporated into neural pixels. (*A*) Bode plot of impedance versus frequency. The impedance magnitude is an average of seven electrodes. Black squares and red dots are the averaged impedance values while the OEIP is off and while K^+ is delivered (1-μA delivery current), respectively. (*B*) Time trace at a single recording site during GABA delivery (60 s < *t* < 120 s) through the sensing electrode to the ACSF target solution.

electrode, which was located adjacent to the MEA (Fig. S3). Moreover, due to multiple recording sites, it is possible to access different forms of activity across the tissue. After *ca.* 1 min of GABA delivery, epileptiform discharges were abolished. Assuming that the delivery is equally distributed between the 32 outlets of the device, 1 μA of supply current yields a delivery rate of 0.3 pmol·s^{-1} per outlet; this corresponds to a local concentration change of 25 μM at a distance of 400 μm from a single pump outlet (18, 21) after 60 s, and is within the known range for GABA to suppress hyperactivity (26) [injection of 250 μM of GABA in the ACSF-filled bath directly on top of the tissue stopped the hyperactivity almost instantaneously (Fig. S4)]. Previous experiments demonstrated local delivery with OEIPs (ref. 22 and Fig. S5), and local control of hippocampal networks with a similar device geometry (21). Taken together, these results demonstrate that the neural pixel system can effectively control the activity of a given network via OEIP delivery, while simultaneously allowing monitoring via the integrated electrodes of both hyperactivity and real-time biological response to OEIP operation.

Because GABA is an acid and is transported by the OEIP in its fully protonated form (charge +1), each GABA molecule will release a proton once delivered to the biological system. Therefore, to verify that the observed abolishment of of epileptiform discharges was solely due to GABA delivery, and not to proton delivery, or to the applied potentials and ionic currents, a control experiment delivering protons was performed. The reservoir was filled with aqueous HCl solution, and the target region contained the hippocampus exhibiting hyperactivity. The same current was sourced to the OEIP as for the GABA delivery experiments; however, we did not observe any significant change in the electrode

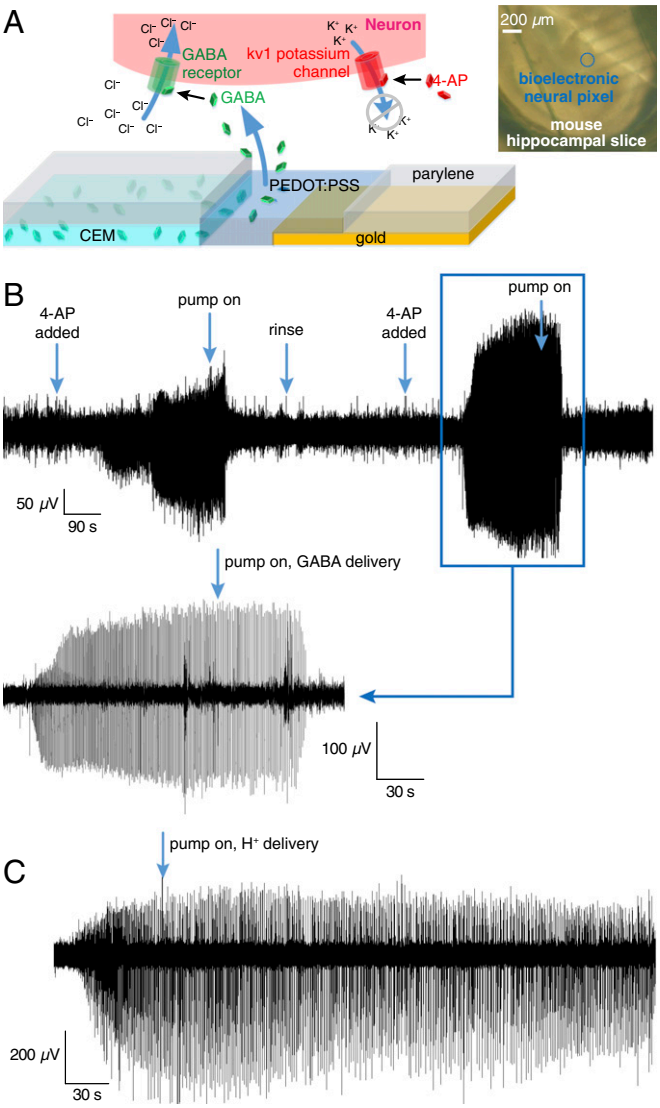

Fig. 4. Epileptiform activity simultaneously recorded and inhibited by a single neural pixel. (*A*) Biochemical pathway for reducing 4-AP-induced epileptiform activity via GABA delivery. (*Inset*) A mouse hippocampal slice positioned on an array of bioelectronic neural pixels. (*B*) Epileptiform activity of a complete mouse hippocampal preparation was recorded from a single pixel before and during GABA delivery to the same pixel. Large events are seen at the beginning of the recording ~100 s after introducing 4-AP to the bath. Approximately 60 s after the OEIP is switched on, the epileptiform activity stops. This cycle is repeated twice by rinsing the bath with ACSF and treating the tissue with 4-AP. (*C*) Response of recording electrodes to delivery of H^+. H^+ delivery has no observable effect on epileptiform activity. The recorded signal is from the epileptic mouse hippocampal neurons upon delivery of H^+ from the OEIP outlets. The activity does not stop when the source reservoir contains HCl and ion pump is operated under the same conditions as with GABA delivery experiment. Negative control denotes delivery of H^+ only. Epileptiform activity was not observed to change.

recordings upon delivery of H^+ (Fig. 4*C*). This result shows that neither proton delivery nor ionic currents (which could cause electrical stimulation) blocked the pathological activity, but that the release of GABA was necessary to stop epileptiform activity.

Discussion

In the present work, we have demonstrated electrophysiological sensing and chemical stimulation from a single multifunctional "neural pixel." This is a necessary advancement to achieve highly localized feedback-regulated therapies with future devices. We have previously shown that we could deliver GABA with an OEIP to stop epileptiform activity in a tissue slice (21). In those experiments, the recording electrode was a tungsten electrode positioned in the tissue slice in the vicinity of an OEIP outlet. In this work, we suppress the need to align this external recording electrode with the outlets of the OEIP. Instead, delivery occurs through the sensing electrodes, ensuring colocalization of recording and stimulation, and eliminating cumbersome experimental setup. The integrated sensing and delivery device stopped externally induced epileptiform activity of a hippocampus by delivering the inhibitory neurotransmitter GABA at the exact sites where epileptic activity was recorded. The low impedance of the conducting polymer electrodes allowed for high signal-to-noise ratio recordings of physiological activity at the site of GABA delivery. To efficiently treat an epileptic event, the delivery of GABA should occur as soon as any signs of seizure appear.

Many studies have shown local release of compounds using microfluidics, for example, refs. 27–29, to name a few. Microfluidics have the ability to deliver any soluble compound, but such delivery in a carrier fluid induces convection, which risks disrupting fragile biochemical microenvironments. Microfluidic systems also typically require complex setups of valves and pumps. Other groups have demonstrated electrically controlled convection-free delivery systems, for example, refs. 16 and 30, that rely on redox switching of conducting polymers to release embedded compounds. However, these systems are typically limited in the amount of deliverable compound, a release rate that decreases over time, and a poor on–off ratio. The OEIP-based delivery built into the neural pixel system is electrically controlled, induces no convection, includes a reservoir to increase the deliverable amount, and exhibits a low diffusive off-leakage because of the relatively large distance between the reservoir and the delivery points (On–Off Switching and Leakage in OEIPs).

Although the electrical signals that turn on the OEIP can be initiated nearly instantaneously, the time required to stop the epileptiform activity after starting GABA delivery was about 60 s. For some applications, this speed may need to be significantly faster. OEIP dynamics are largely governed by the distance that ions must traverse from the source electrolyte to the delivery points. In the present geometry, this length is on the scale of several millimeters. We are thus developing devices with significantly faster turn-on by arranging delivery vertically through a thin CEM film, thereby reducing the effective ion path length to hundreds of nanometers. Likewise, the pixel dimensions in the device described above were 20 × 20 μm, with the 32-electrode array spanning several hundred microns; this is already on the approximate scale of single neurons and local neuronal circuits, respectively. Although miniaturization is feasible (but difficult), increasing these dimensions to fit different therapeutic targets is also possible.

Another limitation with the present neural pixel system is that it delivers ions simultaneously at the 32 outlets, where each outlet is colocalized with a sensing electrode. An addressable pixel array, where each sensing/delivery site could be individually controlled, would thus be a significant improvement. Such a system would make it possible to record from an array of electrodes, and then to selectively turn on the delivery at the sites where, for example, epileptiform activity is recorded. A future device, with individually addressable release sites and colocalized recording electrodes, could also be used as an in vitro tool to precisely quantify the kinetics of specific neurochemical signaling. Furthermore, such individually addressed neural pixels could enable multiple connections to a single neuron, similar to the way biological neurons connect with each other. In this way, the dynamics of multiple neural connections could be studied with unprecedented detail.

The lifetime of our device depends on the electrochemical capacity of the electrodes and the delivery rate required for the application. For an in vitro study like the one above, lasting only hours, electrode capacity is not an issue, especially because consumed electrodes can easily be replaced by fresh, free-standing electrodes dipped into the electrolytes. For an implantable in vivo device, however, electrode capacity is crucial. Larger or more three-dimensionally structured electrodes and delivery in short pulses would increase the lifetime. Another solution would be to incorporate an ion diode-based current rectifier, so that the electrodes could be electrochemically "recycled," increasing the lifetime substantially (31). Likewise, for in vivo applications, the device could be built on flexible substrates, e.g., parylene C, and wrapped onto a tissue, but additional fabrication issues such as long-term mechanical and lamination stability must also be considered; this is something we have not yet explored, however. For applications deeper inside the tissue or organ of interest, neural pixel systems could be constructed into implantable probes, a technique already demonstrated for basic OEIPs (19, 22).

The ability to sense electrophysiological signals and deliver neuroactive compounds at the same location represents a first step in constructing a closed-loop feedback system, capable of monitoring neuronal activity and adjusting local release of neurotransmitters accordingly. Indeed, the system presented above only requires minor modification to the control software to explore this functionality. Such a closed-loop system could be used, for example, in epilepsy treatment, to predict or detect an epileptic seizure at an early stage and intervene by delivering inhibitory neurotransmitters. The feedback system would make it possible to stop seizures with a minimal amount of drugs, because the drug release could be stopped as soon as the inhibitory effect is observed.

Methods

Device Fabrication. The 3 × 1 inch glass slides were cleaned by sonication in soap/water mixture and acetone/IPA mixture. For patterning gold, a photoresist, S1813 (Shipley), was spin-cast on the glass slide, exposed to UV light using an SUSS MJB4 photolithography UV-mask aligner, and developed using MF-26 developer. Titanium and gold (100 nm) were evaporated (Alliance Concept EVA450) and patterned using lift-off in acetone. On top of a layer cast from soap/water solution, 1.5 μm of parylene C was deposited using a Specialty Coating Systems Labcoater 2; 4 μm of photoresist AZ9260 was then patterned and etched (300 W, 50 cm^3/min of O_2, 5 min) using an Oxford 80 plus plasma etcher. A solution of 3-glycidoxypropyltrimethoxysilane (GOPS, 5 wt%) in a water:ethanol mixture (1:19) was spin-coated to improve the adhesion of the PSSA-co-MA on glass. After 15 min, the substrates were rinsed in ethanol to remove excess GOPS. Then the substrates were baked at 110 °C for 20 min. PSSA-co-MA (5 wt% in a water:1-propanol mixture, 1:1) was mixed with polyethylene glycol (3 wt%, molecular weight 400 $g \cdot mol^{-1}$) for cross-linking, and then deposited by spin casting at 2,000 rpm to obtain a thickness of 300 nm. The film was baked at 110 °C for 1 h. The sacrificial parylene C layer was peeled off to complete the patterning of PSSA-co-MA. Another layer of parylene C was deposited, reaching a final thickness of 2 μm, with the use of an adhesion promoting silane. A soap solution (1 wt% in water) was spun and followed by a subsequent parylene C deposition (2 μm). Finally, the source/target PEDOT:PSS was patterned with the insulating parylene C using photolithography and a sacrificial peel-off step. A thick layer of AZ9260 (MicroChemicals) photoresist was cast, baked, and exposed using a SUSS MJB4 contact aligner, followed by reactive ion etching in an O_2 plasma (160 W, 50 cm^3/min of O_2, 15 min) using an Oxford 80 plus plasma etcher. For the preparation of the PEDOT:PSS films, 19 mL of aqueous dispersion (PH 1000 from H.C. Starck) was mixed with 1 mL of ethylene glycol, 50 μL

of dodecyl benzene sulfonic acid, and 1 wt% of GOPS, and the resulting dispersion was spin-coated at 650 rpm, soft-baked at 100 °C for 60 s, and spun-cast at 650 rpm to attain thicker PEDOT:PSS films. The film is patterned by peel-off of the top parylene C film and subsequently baked at 140 °C for 1 h and immersed in deionized water to remove any excess low molecular weight compounds. The reservoir chambers, cut from cured polydimethylsiloxane, were affixed to the source (reservoir) and target (bath) areas.

Device Characterization. Impedance spectra of the electrodes were measured using an Autolab potentiostat equipped with a frequency response analyzer (FRA) module. Commercially available Ag/AgCl and Pt electrodes were used as the counter and reference electrodes. The applied voltage was 0.01 V, and the electrolyte solution was aqueous 0.1 M NaCl(aq). The contacts of the OEIP were connected to a Keithley 2400 source/measure unit, and constant current (1 μA or lower) was sourced and voltage was measured using customized LabVIEW software. Electrode recordings were obtained using a commercially available voltage recording setup, RHD2000 Evaluation System. As the reference electrode, a grounded Ag/AgCl electrode was immersed into the target electrolyte. The recordings were acquired at a 20-kHz sampling rate and analyzed using MATLAB (Mathworks)-based software with a low-pass filter of 1 kHz and were down-sampled by 500.

Electrical Recording Data Acquisition. Electrode recordings were obtained using a commercially available voltage recording setup, RHD2000 Evaluation System (Intan Technologies) (Fig. S2). A 3D printed sample holder was fabricated, containing gold-coated pins in contact with the 32 gold electrode pads of the device. As the reference electrode, a grounded Ag/AgCl electrode was immersed into the target reservoir containing the brain slice. Recordings were acquired at a 20-kHz sampling rate and analyzed using MATLAB (Mathworks)-based software with a low-pass filter of 1 kHz and were down-sampled by 500.

Hippocampus Preparation. All protocols have been approved by the Institutional Animal Care and Use Committee of INSERM. All experiments were repeated twice on different biological samples. After decapitation of anesthetized mice, brains were rapidly extracted (postnatal day 14 through 18). In a chilled and perfused bath, the brain was cut into the left and right hemisphere, and the complete hippocampus, including the septum, was extracted from each hemisphere. This preparation maintains the whole 3D hippocampal architecture, preserving cellular and axonal integrity (32, 33). Freshly extracted preparations were placed in a chamber and perfused with oxygenated (95% O_2/5% CO_2) ACSF (126 mM NaCl, 3.5 mM KCl, 2 mM $CaCl_2$, 1.3 mM $MgCl_2$, 1.2 mM NaH_2PO_4, 26.2 mM $NaHCO_3$, and 10 mM glucose). They were maintained in the chamber at room temperature and allowed to recover for 1 h before experimental use. After this period of recovery, preparations were transferred with a pipette to the surface of the integrated sensing/delivery device. The chamber containing the hippocampus was continuously perfused with oxygenated ACSF warmed at 33 °C. Tungsten electrodes (with a tip resistance of 1 MΩ to 3 MΩ) were positioned on top of the OEIP outlets/electrode openings. External electrode recordings were made with a World Precision Instruments DAM80 AC amplifier, and were acquired using an analog-to-digital converter (Digidata 1322B; Molecular Devices). Analysis was performed using using Clampfit (Molecular Devices)- or MATLAB (Mathworks)-based software.

ACKNOWLEDGMENTS. We thank Gaelle Rondeau and the staff of the clean room in Centre Microelectronique de Provence (CMP) for technical support during fabrication. The research leading to these results has received funding from the European Union's Seventh Framework Programme (FP7/2007-2013) under Grant Agreement 602102 (EPITARGET) and Initiative of Excellence Aix-Marseilles project MIDOE (A_M-AAP-ID-13-24-130531-16.31-BERNARD-HLS). Funding was also provided by the Swedish Innovation Office (2010-00507), the Swedish Research Council (621-2011-3517), and the Knut and Alice Wallenberg Foundation (KAW Scholar, 2012.0302). The authors also thank the National Science Foundation Grant DMR-1105253 for partial support of this work, the French National Research Agency (ANR) through the project PolyProbe (ANR-13-BSV5-0019-01), Fondation pour la Recherche Médicale under Grant Agreements DBS20131128446 and ARF20150934124, Fondation de l'Avenir, the Önnesjö Foundation, the Region Provence-Alpes-Côte d'Azur, and Microvitae Technologies. J.R. and L.K. acknowledge support from Marie Curie Fellowships. The fabrication of the device was performed, in part, at CMP.

1. Kringelbach ML, Jenkinson N, Owen SLF, Aziz TZ (2007) Translational principles of deep brain stimulation. *Nat Rev Neurosci* 8(8):623–635.
2. Rogawski MA, Löscher W (2004) The neurobiology of antiepileptic drugs. *Nat Rev Neurosci* 5(7):553–564.
3. Bialer M, White HS (2010) Key factors in the discovery and development of new antiepileptic drugs. *Nat Rev Drug Discov* 9(1):68–82.
4. Löscher W, Potschka H (2005) Drug resistance in brain diseases and the role of drug efflux transporters. *Nat Rev Neurosci* 6(8):591–602.
5. Higgins CF (2007) Multiple molecular mechanisms for multidrug resistance transporters. *Nature* 446(7137):749–757.
6. Kwan P, Brodie MJ (2001) Neuropsychological effects of epilepsy and antiepileptic drugs. *Lancet* 357(9251):216–222.
7. Perucca P, Gilliam FG (2012) Adverse effects of antiepileptic drugs. *Lancet Neurol* 11(9):792–802.
8. Wolinsky JB, Colson YL, Grinstaff MW (2012) Local drug delivery strategies for cancer treatment: Gels, nanoparticles, polymeric films, rods, and wafers. *J Control Release* 159(1):14–26.
9. Cook MJ, et al. (2013) Prediction of seizure likelihood with a long-term, implanted seizure advisory system in patients with drug-resistant epilepsy: A first-in-man study. *Lancet Neurol* 12(6):563–571.
10. Cogan SF (2008) Neural stimulation and recording electrodes. *Annu Rev Biomed Eng* 10(1):275–309.
11. Buzsáki G, Anastassiou CA, Koch C (2012) The origin of extracellular fields and currents—EEG, ECoG, LFP and spikes. *Nat Rev Neurosci* 13(6):407–420.
12. Ludwig KA, Uram JD, Yang J, Martin DC, Kipke DR (2006) Chronic neural recordings using silicon microelectrode arrays electrochemically deposited with a poly(3,4-ethylenedioxythiophene) (PEDOT) film. *J Neural Eng* 3(1):59–70.
13. Ludwig KA, et al. (2011) Poly(3,4-ethylenedioxythiophene) (PEDOT) polymer coatings facilitate smaller neural recording electrodes. *J Neural Eng* 8(1):014001.
14. Venkatraman S, et al. (2011) In vitro and in vivo evaluation of PEDOT microelectrodes for neural stimulation and recording. *IEEE Trans Neural Syst Rehabil Eng* 19(3):307–316.
15. Green RA, Lovell NH, Wallace GG, Poole-Warren LA (2008) Conducting polymers for neural interfaces: Challenges in developing an effective long-term implant. *Biomaterials* 29(24-25):3393–3399.
16. Abidian MR, Kim D-H, Martin DC (2006) Conducting-polymer nanotubes for controlled drug release. *Adv Mater* 18(4):405–409.
17. Sessolo M, et al. (2013) Easy-to-fabricate conducting polymer microelectrode arrays. *Adv Mater* 25(15):2135–2139.
18. Tybrandt K, et al. (2009) Translating electronic currents to precise acetylcholine-induced neuronal signaling using an organic electrophoretic delivery device. *Adv Mater* 21(44):4442–4446.
19. Simon DT, et al. (2009) Organic electronics for precise delivery of neurotransmitters to modulate mammalian sensory function. *Nat Mater* 8(9):742–746.
20. Isaksson J, et al. (2007) Electronic control of Ca^{2+} signalling in neuronal cells using an organic electronic ion pump. *Nat Mater* 6(9):673–679.
21. Williamson A, et al. (2015) Controlling epileptiform activity with organic electronic ion pumps. *Adv Mater* 27(20):3138–3144.
22. Jonsson A, et al. (2015) Therapy using implanted organic bioelectronics. *Sci Adv* 1(4):e1500039.
23. Simon DT, et al. (2015) An organic electronic biomimetic neuron enables auto-regulated neuromodulation. *Biosens Bioelectron* 71(0):359–364.
24. Strathmann H (2004) *Ion-Exchange Membrane Separation Processes* (Elsevier, New York).
25. Jones R (2012) Neurotransmission: GABA calls stop in the striatum. *Nat Rev Neurosci* 13(12):815.
26. Jones MV, Westbrook GL (1995) Desensitized states prolong GABAA channel responses to brief agonist pulses. *Neuron* 15(1):181–191.
27. Hendricks JL, Chikar JA, Crumling MA, Raphael Y, Martin DC (2008) Localized cell and drug delivery for auditory prostheses. *Hear Res* 242(1-2):117–131.
28. Jeong J-W, et al. (2015) Wireless optofluidic systems for programmable in vivo pharmacology and optogenetics. *Cell* 162(3):662–674.
29. Minev IR, et al. (2015) Electronic dura mater for long-term multimodal neural interfaces. *Science* 347(6218):159–163.
30. Svirskis D, Travas-Sejdic J, Rodgers A, Garg S (2010) Electrochemically controlled drug delivery based on intrinsically conducting polymers. *J Control Release* 146(1):6–15.
31. Gabrielsson EO, Janson P, Tybrandt K, Simon DT, Berggren M (2014) A four-diode full-wave ionic current rectifier based on bipolar membranes: Overcoming the limit of electrode capacity. *Adv Mater* 26(30):5143–5147.
32. Khalilov I, et al. (1997) A novel in vitro preparation: The intact hippocampal formation. *Neuron* 19(4):743–749.
33. Davies ML, Kirov SA, Andrew RD (2007) Whole isolated neocortical and hippocampal preparations and their use in imaging studies. *J Neurosci Methods* 166(2):203–216.